Developmental Biology
Neuroscience

Activity-dependent synapse elimination requires caspase-3 activation

Reviewed Preprint
v2 • March 20, 2025
Revised by authors

Reviewed Preprint
v1 • October 18, 2024

Zhou Yu, **Andrian Gutu**, **Namsoo Kim**, **Erin K O'Shea**

Janelia Research Campus, Howard Hughes Medical Institute, Ashburn, United States • Current address: Brigham and Women's Hospital, Harvard Medical School, Boston, United States

eLife Assessment

This study presents an **important** finding on the involvement of a Caspase 3-dependent pathway in the elimination of synapses for retinogeniculate circuit refinement and eye-specific territory segregation. This work fits well with the concept of "synaptosis" which has been proposed in the past. The evidence supporting the claims of the authors is **convincing**, demonstrating that caspase-3 activation is essential for microglial elimination of synapses during both brain development and neurodegeneration. The work will be of interest to investigators studying cell death pathways, neurodevelopment, and neurodegenerative disease.

https://doi.org/10.7554/eLife.101779.2.sa2

Abstract

During brain development, synapses are initially formed in excess and are later eliminated in an activity-dependent manner. Weak synapses are preferentially removed, but the mechanism linking neuronal activity to synapse removal is unclear. Here we show that, in the developing mouse visual pathway, inhibiting synaptic transmission induces postsynaptic activation of caspase-3. Caspase-3 deficiency results in defects in synapse elimination driven by both spontaneous and experience-dependent neural activity. Notably, caspase-3 deficiency blocks activity-dependent synapse elimination, as evidenced by reduced engulfment of inactive synapses by microglia. Furthermore, in a mouse model of Alzheimer's disease, caspase-3 deficiency protects against synapse loss induced by amyloid-β deposition. Our results reveal caspase-3 activation as a key step in activity-dependent synapse elimination during development and synapse loss in neurodegeneration.

Main Text

Synapse elimination is the process in which excess synapses formed early during brain development are subsequently eliminated to form mature circuits (1–3). The outcome of synapse elimination depends on both spontaneous and experience-driven neural activity, with less active synapses being preferentially removed (2, 4, 5). However, the molecular mechanisms that connect neuronal activity to synapse elimination remain unclear. Previous studies have proposed that microglia and astrocytes, two major glial cell types of the brain, mediate activity-dependent synapse elimination by engulfing weak synapses (6–14), but it is unclear how glia can detect the "strength" of a synapse. A recent study proposed a molecular mechanism for activity-dependent synapse elimination in which the JAK2-STAT1 pathway is activated in inactive callosal projection neurons and regulates the removal of synapses and axons (15). However, the JAK-STAT pathway canonically functions through transcriptional regulation (16), which affects entire cells. If not all synapses made by a neuron are destined for removal (3), activation of the JAK2-STAT1 pathway alone may not provide sufficient elimination specificity. Therefore, other unidentified, locally-effective mechanisms likely exist that confer elimination specificity at the synapse level.

Caspase-3 is a protease crucial for the execution of apoptosis (17). In hippocampal neurons, transient activation of caspase-3 is required for long-term depression (LTD), a form of synaptic plasticity that induces long-lasting decreases in synaptic strength (18). Caspase-3 activation in apoptotic cells is also known to lead to the clearance of these cells by phagocytes (19, 20). These findings led us to hypothesize that caspase-3 may link synapse weakening with synapse removal by glia. Although caspases were previously implicated in dendrite pruning in metamorphosis, degeneration-like axon elimination, and the regulation of hippocampal spine density (21–24), the role of caspase-3 in synapse elimination in response to neural activity was not clear. In this work, we identify caspase-3 as a key molecule that is activated in postnatal development in dendritic compartments upon synaptic weakening and is necessary for elimination of weak synapses by microglia. Furthermore, we discovered that caspase-3 deficiency protects against amyloid-β-induced synapse loss in a mouse model of Alzheimer's disease, highlighting its significance not only in developmental synapse elimination but also in adult neurodegenerative diseases.

Tetanus toxin expression inactivates retinogeniculate synapses

We chose the mouse retinogeniculate visual pathway as a model system to study synapse elimination (25). In mice, retinal ganglion cells (RGCs) in each eye send out axons to form retinogeniculate synapses with relay neurons in the dorsal lateral geniculate nuclei (dLGN) of the thalamus on both sides of the brain (Fig. S1) (25). The majority of RGC axons from each eye innervate the contralateral (on the side opposite to the originating eye) dLGN while a smaller fraction innervate the ipsilateral (on the same side as the originating eye) dLGN (Fig. S1) (25). Regions in each dLGN innervated by the two eyes initially overlap but later segregate into eye-specific territories (Fig. S1). This segregation process is a hallmark of retinogeniculate pathway development at the morphological level and depends on synapse elimination and spontaneous RGC activity (25–27).

To investigate the role of caspase-3 in activity-dependent synapse elimination, we first needed to establish a method that could manipulate the strength of a subset of retinogeniculate synapses. For this purpose, we used adeno-associated-virus (AAV) to deliver a construct expressing tetanus toxin light chain (TeTxLC) under the control of the neuron-specific human synapsin promoter (AAV-hSyn-TeTxLC) (**Fig. 1A**) (28). *In utero* intraocular injection of AAV-hSyn-TeTxLC at embryonic day 15 (E15) leads to TeTxLC expression in RGCs by the time of birth, blocking neurotransmitter

release at retinogeniculate synapses by cleaving synaptobrevin and leading to synapse inactivation (28, 29). To label RGC axons and facilitate quantification, we co-injected AAVs that express fluorescent proteins (mTurquiose2, eGFP, or tdTomato, depending on the experiment) as anterograde tracers (**Fig. 1A**). These AAVs expressing fluorescent proteins also served as controls for eye injections.

To validate the efficacy of our synapse inactivation method, we injected AAV-hSyn-TeTxLC into the right eye of wildtype E15 embryos and analyzed the segregation of eye-specific territories at postnatal day 8 (P8), when the segregation process is largely complete (25). To quantify the overlap between eye-specific territories in an unbiased manner, we applied a set of increasing thresholds to signals from both eyes (Fig. S2) (30). For each threshold, we calculated a percentage overlap value as the ratio of the dLGN area with signals from both eyes to the total dLGN area (Fig. S2 and Fig. S3). Consistent with previous results (26, 27), inactivating right eye-associated retinogeniculate synapses led to contraction of right eye-specific territories and expansion of left eye-specific territories relative to control animals (Fig. S3A and S3B). Importantly, segregation of eye-specific territories in TeTxLC-injected mice was significantly defective (Fig. S3C and S3D), confirming that our method potently inactivated synapses and perturbed activity-dependent refinement of the retinogeniculate pathway.

Synapse inactivation induces postsynaptic caspase-3 activity

Is caspase-3 activated in response to synapse weakening? To address this question, we injected AAV-hSyn-TeTxLC into the right eyes of E15 embryos and looked for caspase-3 activation in dLGNs of TeTxLC-injected mice at the age of P5 (a time when synapse elimination is most active) (**Fig. 1A**) (7, 25). We used immunohistochemistry against the cleaved and active form of caspase-3 to detect caspase-3 activity in the dLGN area (17). If synapse inactivation leads to caspase-3 activation, we would expect higher levels of caspase-3 activity in dLGNs with more inactivated synapses (**Fig. 1A**). In agreement with this hypothesis, caspase-3 activity in left dLGNs of TeTxLC-injected animals (dLGNs with the most inactivated synapses) was significantly higher compared to that in right dLGNs of the same animals (dLGNs with intermediate amount of inactivated synapses) (**Fig. 1B**, **1C**, and **1E**) and compared to that in dLGNs of animals receiving control injections in the right eyes (dLGNs with no inactivation) (**Fig. 1B**, **1D**, and **1E**). Reassuringly, caspase-3 activities in left and right dLGNs of control animals were comparable (**Fig. 1E**), despite injections being administered only in the right eyes. This suggests that surgical manipulation and viral transduction had no measurable contribution to caspase-3 activation. These findings support the model that inactivation of retinogeniculate synapses leads to caspase-3 activation.

Does inactivation of retinogeniculate synapses activate caspase-3 pre-synaptically in RGCs or post-synaptically in dLGN relay neurons? Caspase-3 activity in dLGNs of TeTxLC-injected mice was present either as discrete, punctate signals (**Fig. 1F**) or as staining of entire cells (**Fig. 1B** and Fig. S4Bi-iii). Both types of signals were more abundant in dLGNs with strong synapse inactivation than in control dLGNs (**Fig. 1B**, **1D** and **1F**). Intriguingly, punctate caspase-3 activity was not found within TeTxLC-expressing RGC axons (**Fig. 1G**). Instead, punctate caspase-3 activity closely juxtaposed inactivated axon terminals (**Fig. 1G**) and co-localized with the dendritic marker MAP2 (Fig. S4A). In the case where caspase-3 was activated in entire cells, the cells were positive for the neuronal marker NeuN (Fig. S4C) and possessed relatively large round somas and multipolar dendritic arbors (Fig. S4Bi-iii), all of which are characteristics of dLGN relay neurons (31, 32). These observations suggest that caspase-3 activation triggered by synapse inactivation occurs predominantly in the dendritic compartments of dLGN relay neurons that are postsynaptic to the inactivated synapses.

Although morphologically distinct, localized and whole-cell caspase-3 activity may be mechanistically linked. In support of this, we observed transitional states of caspase-3 activation where multiple dendrites of a relay neuron were positive for active caspase-3 without the cell

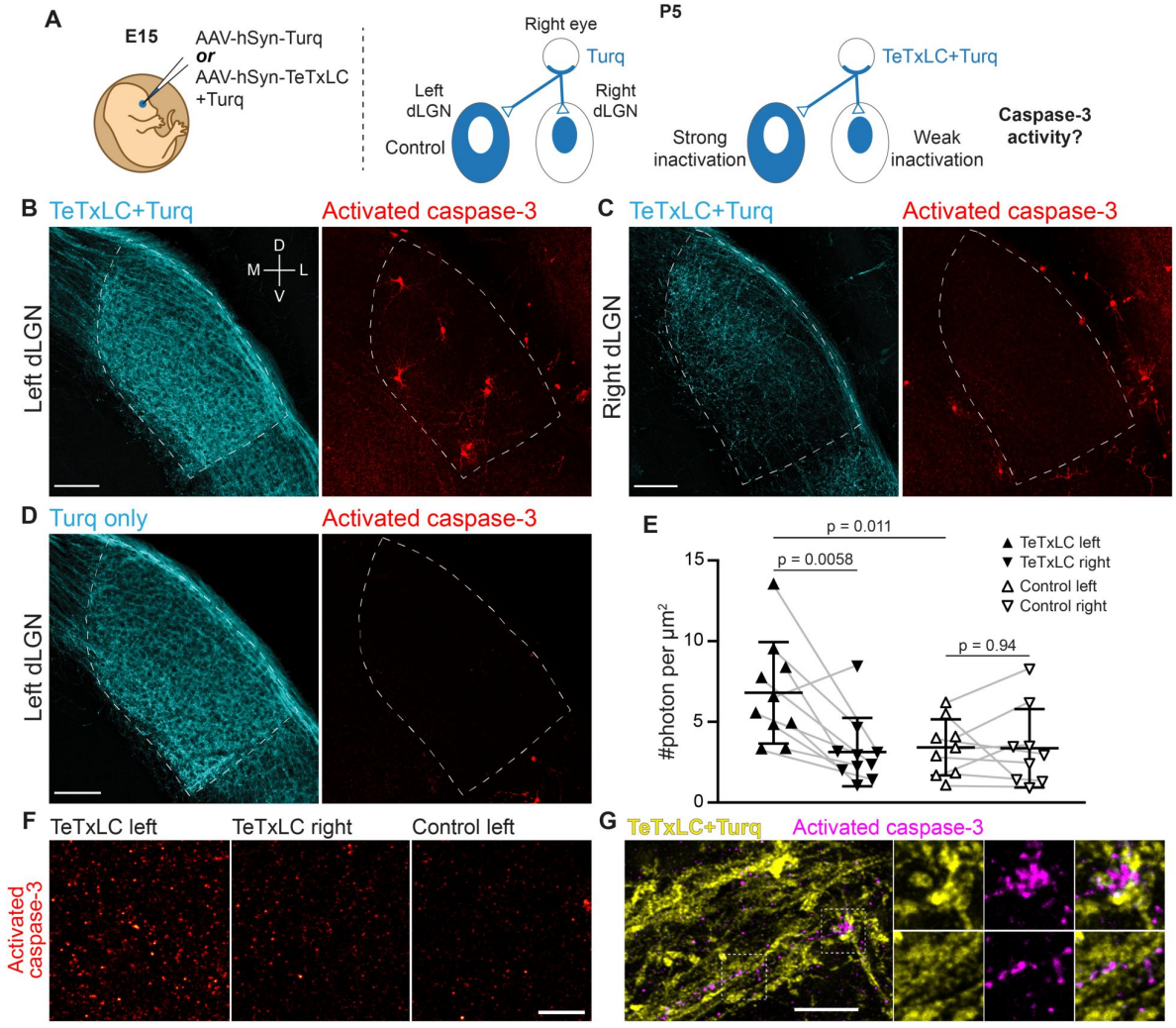

Figure 1.

Inactivation of retinogeniculate synapses induces caspase-3 activity.

(**A**) Schematics of experimental setup. AAVs expressing tetanus toxin light chain (TeTxLC) and/or mTurquiose2 (Turq) were injected into the right eye of E15 mice (left). By P5, retinogeniculate synapses in dLGN were inactivated to varying extents depending on injection and side (right). (**B**-**D**) Confocal images of Turq (left panels) and activated caspase-3 (right panels) in left dLGN (**B**) and right dLGN (**C**) of a TeTxLC-injected P5 animal and in left dLGN of a control P5 animal (**D**). Dotted lines delineate dLGN boundaries. Only signals within dLGNs were analyzed. Images from the same fluorescent channel were adjusted to the same contrast. The compass in **B** marks tissue orientation. Scale-bars: 100 µm. D, dorsal; V, ventral; M, medial; L, lateral. (**E**) Quantification of caspase-3 activity in indicated dLGNs. Activated caspase-3 signals in each dLGN (highlighted areas in **B**-**D**) were summed and normalized to dLGN area. Each point represents the result from one dLGN. Data from two dLGNs of the same animal were paired for analysis (grey lines). n=10 for TeTxLC-injected animals and n=9 for control animals. Mean and standard deviation (S.D.) are shown. P-values were calculated from two-tailed t-tests (paired when applicable). (**F**) Example images showing punctate caspase-3 activities in ventral-medial regions of indicated dLGNs. Images were adjusted to the same contrast. Scale-bar: 20 µm. (**G**) High-resolution images of dLGN showing TeTxLC-expressing RGC axons (yellow) and activated caspase-3 (magenta). Two regions of interest (dotted squares) are magnified to illustrate that caspase-3 activity was found juxtaposing TeTxLC-expressing axon terminals but not within them. Scale-bar: 5 µm.

body becoming apoptotic (an example is shown in Fig. S4Biv), suggesting that whole-cell caspase-3 activation may arise from accumulation of local caspase-3 activity. Such transitions might be particularly relevant in dLGNs that receive the majority of TeTxLC-expressing axons, as systematic silencing of synapses could lead to widespread caspase-3 activation in the postsynaptic neuron, potentially overwhelming negative regulatory mechanisms that normally keep caspase-3 activation localized (24, 33–35). While our data cannot determine which form of caspase-3 activation plays a more significant role in the normal development of the visual pathway, the infrequent occurrence of whole-cell caspase-3 activation in control dLGNs (**Figure 1D**) -- which undergo normal synapse elimination -- suggests that localized caspase-3 activation is necessary to drive synapse elimination under physiological conditions.

Caspase-3 activation at weak synapses requires the presence of strong synapses

Previous experiments have manipulated RGC neuronal activities and demonstrated that, regardless of the absolute level of RGC activity, the dLGN territory of less active RGCs always contracted relative to that of more active RGCs (26, 27). This observation suggests that the outcome of synapse elimination is driven by competitive interactions between strong and weak synapses. Consistent with this idea, a recent study demonstrated that elimination of weak synapses in callosal projections occurred only when other strong synapses are present (28, 36).

To test if caspase-3 activation at weak synapses requires the presence of strong synapses, we designed two experimental conditions. In the first condition, we inactivated RGCs only in the right eye, leading to the presence of both active (from the left eye) and inactive (from the right eye) synapses in the dLGN (**Fig. 2A**). We termed this condition “single inactivation”. In the second condition, we inactivated RGCs in both eyes, leading to the presence of only inactive synapses in the dLGN (**Fig. 2A**). We termed this condition “dual inactivation”. We also included a control condition where no RGCs were inactivated (**Fig. 2A**). We first confirmed that, in accordance with previous findings (26, 37), segregation of eye-specific territories was disrupted in the dual inactivation condition (Fig. S5A-D). We then measured dLGN caspase-3 activity in control, single, and dual inactivation conditions. Intriguingly, while dLGN caspase-3 activity was significantly higher in the single inactivation condition compared to that in the control (**Fig. 2B** and **2C**), dLGN caspase-3 activity in the dual inactivation condition was not significantly different from that in the control (**Fig. 2B** and **2C**) and was significantly lower than that in the single inactivation condition (**Fig. 2B** and **2C**). Although not reaching statistical significance, dLGN caspase-3 activity on average was still higher in the dual inactivation condition compared to the control (**Fig. 2C**), possibly due to incomplete inactivation of retinogeniculate synapses, or interaction between weak retinogeniculate synapses and strong synapses from other pathways, or additional mechanisms that activate caspase-3 independently of interactions between weak and strong synapses. These results suggest that interaction between weak and strong synapses is required for caspase-3 activation to occur at weak synapses.

Caspase-3 is required for segregation of eye-specific territories

Is synapse inactivation-induced caspase-3 activity important for synapse elimination in the retinogeniculate pathway? To address this question, we investigated whether segregation of eye-specific dLGN territories is defective if caspase-3 activation does not occur. Since we were unable to find a Cre-expressing mouse line that satisfactorily depletes caspase-3 in dLGN relay neurons, we used full-body caspase-3 deficient (*Casp3*$^{-/-}$) mice (38, 39). These mice were backcrossed to congenicity on the C57Bl/6J background and were viable, fertile, and did not exhibit overt abnormalities (39). To measure segregation of eye-specific territories, we injected the eyes of *Casp3*$^{+/+}$ and *Casp3*$^{-/-}$ littermate mice at P9 with fluorophore-conjugated cholera toxin subunit B (CTB), using a different fluorophore for each eye. CTB molecules bind to ganglioside molecules on

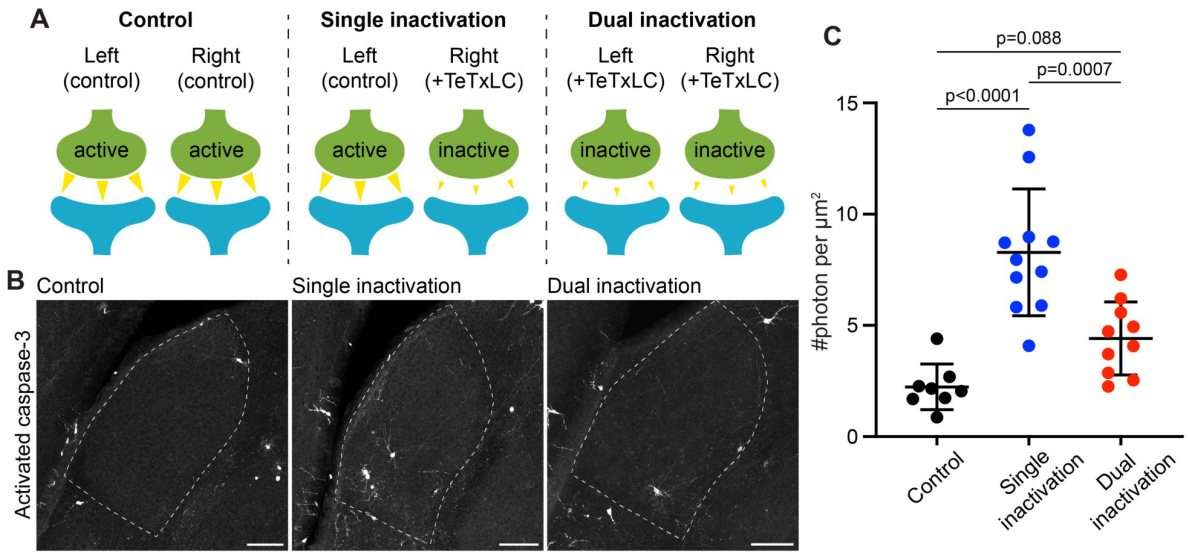

Figure 2.

Caspase-3 activation at weak synapses requires the presence of strong synapses.

(**A**) Schematics illustrating experimental conditions. No synapses are inactivated in the control (left); only synapses from right eyes are inactivated in single inactivation condition (middle); synapses from both right and left eyes are inactivated in dual inactivation condition (right). (**B**) Confocal images of P5 left side dLGNs in the three conditions showing caspase-3 activity in the dLGN. Dotted lines mark dLGN boundaries. Scale-bars: 100 µm. (**C**) Quantification of dLGN caspase-3 activity in the indicated conditions. Caspase-3 activity in each dLGN were summed and normalized to the dLGN area. For the single inactivation condition, values were from left dLGNs only. For the other two conditions, values from both dLGNs were averaged. n=8 animals for control, n=11 animals for single inactivation, and n=10 animals for dual inactivation. Mean and S.D. are shown. P-values were calculated from Tukey's multiple comparison tests.

RGC surfaces and anterogradely label RGC axon terminals (40). At P10, when CTB labeling and eye-specific segregation were complete (25, 30), we collected the brains and imaged eye-specific territories in each dLGN. By visual inspection, eye-specific territories in *Casp3*$^{+/+}$ dLGNs overlapped minimally (**Fig. 3A**). In contrast, *Casp3*$^{-/-}$ dLGNs showed clear defects in the separation of eye-specific territories (**Fig. 3B**) (41). We then quantified eye-specific segregation as described previously (Figure S2) and found that percentage overlap in *Casp3*$^{-/-}$ dLGNs was consistently higher than that in *Casp3*$^{+/+}$ dLGNs across all thresholds (**Fig. 3C and D**). Importantly, the fold difference and statistical significance of the difference in percentage overlap between the two groups of animals increased as the cutoff threshold increased (**Fig. 3D**), suggesting the defects observed in *Casp3*$^{-/-}$ animals cannot be attributed to artifacts generated from background noise.

As RGCs are known to undergo extensive apoptosis during the first week of postnatal development (42, 43), we wondered if caspase-3 deficiency might block RGC turnover and result in more RGC inputs in the dLGN, thereby confounding the overlap analysis. To address this concern, we quantified the density of RGCs in whole-mount retinae using a RGC marker, RBPMS (Fig. S6A) (44). Reassuringly, RGC densities in retinae of *Casp3*$^{+/+}$ and *Casp3*$^{-/-}$ mice were not different (Fig. S6B), indicating that RGC apoptosis still occurred at normal rates in the absence of caspase-3, presumably through redundant mechanisms.

It is also possible that caspase-3 deficiency might confound the overlap analysis by affecting the number of dLGN relay neurons. Therefore, we used NeuN staining to visualized relay neurons in dLGNs of *Casp3*$^{+/+}$ and *Casp3*$^{-/-}$ mice and confirmed that relay neuron density is not significantly altered by caspase-3 deficiency (Figure S7). Notably, this observation indicates that, during normal development, synapse weakening does not induce widespread whole-cell caspase-3 activation in dLGN relay neurons, corroborating the idea that localized caspase-3 activity drives synapse elimination in dLGN. Collectively, our findings suggest that caspase-3 is required for normal segregation of eye-specific territories in dLGN.

Caspase-3 is required for retinogeniculate circuit refinement

Segregation of eye-specific territories in the mouse dLGN occurs prior to eye opening (which happens at ~P13) and relies predominantly on spontaneous RGC activity (25). After eye opening, sensory-dependent RGC activity drives a second phase of refinement at the circuit level (25). At the time of eye opening, each dLGN relay neuron receives numerous weak RGC inputs. With visual experience, a minority of these inputs are strengthened while other weak inputs are eliminated, so that by P30 only a few (typically ≤3) strong RGC inputs innervate each dLGN relay neuron (25).

To test if caspase-3 is required for visual experience-driven circuit refinement, we prepared acute brain slices from P30 *Casp3*$^{+/+}$ and *Casp3*$^{-/-}$ littermate mice and investigated the electrophysiological properties of retinogeniculate synapses (Fig. S8A) (45, 46). We stimulated the optic tract while recording both AMPA receptor (AMPAR)- and NMDA receptor (NMDAR)-mediated excitatory postsynaptic currents (EPSCs) in dLGN relay neurons (Fig. S8A and **Fig. 4A-B**). By gradually increasing the stimulation intensity on the optic tract, we recruit individual RGC axons in a serial manner (Fig. S8A). Excitation of each RGC axon triggers a step increase in the EPSC amplitude (Fig. S8A), allowing us to infer RGC input numbers by counting steps in EPSC response curves (**Fig. 4C** and S9A). In agreement with previous studies, retinogeniculate circuits in *Casp3*$^{+/+}$ animals were refined, with dLGN relay neurons most frequently receiving 2 strong RGC inputs, and the great majority of neurons receiving no more than 3 inputs (**Fig. 4A**, **4C** and S9A). In contrast, RGC input counts of dLGN relay neurons in *Casp3*$^{-/-}$ animals followed a long-tailed distribution that was significantly right-shifted from that of *Casp3*$^{+/+}$ animals (**Fig. 4C** and S9A). The majority of *Casp3*$^{-/-}$ relay neurons received more than 3 inputs (**Fig. 4B-C** and S9A), and many inputs elicited only small increments in EPSC amplitude (**Fig. 4B**). Additionally, we examined maximum EPSC amplitude (Fig. S9B-C), AMPAR-EPSC to NMDAR-EPSC ratio (Fig.

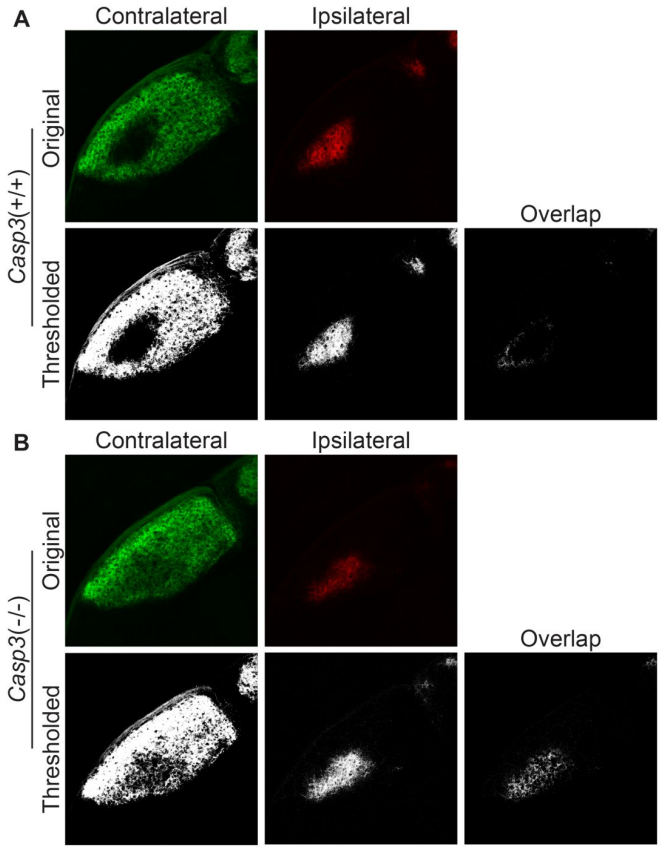

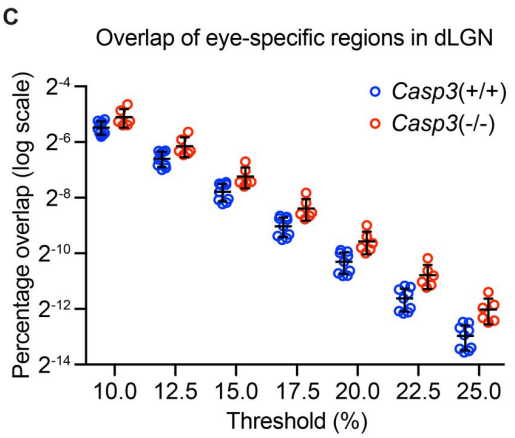

D

Threshold (%)	*Casp3*(+/+) mean	*Casp3*(-/-) mean	p-value
10.0	0.0224	0.0290	0.027
12.5	0.0103	0.0141	0.016
15.0	0.00453	0.00662	0.0095
17.5	0.00192	0.00298	0.0056
20.0	0.00079	0.00131	0.0034
22.5	0.00032	0.00057	0.0021
25.0	0.00012	0.00024	0.0015

Figure 3.

Caspase-3 is required for segregation of eye-specific territories.

(**A**-**B**) Representative confocal images of retinogeniculate inputs in the dLGN of P10 wild-type (**A**) and *Casp3*$^{-/-}$ (**B**) mice. Contralateral inputs are labeled with AlexaFlour488 (AF488) conjugated cholera toxin subunit B (CTB) and ipsilateral inputs with AF594-CTB. Original images were thresholded into 0-or-1 images using the Otsu method (34), and the overlap between thresholded contralateral and ipsilateral inputs is shown. (**C**) Percentage overlap between eye-specific territories in wildtype and *Casp3*$^{-/-}$ mice under a series of increasing signal cutoff thresholds. Note that the percentage overlap is plotted on a log scale. Each circle represents one animal. Mean and S.D. are shown. n=9 for wildtype mice and n=6 for *Casp3*$^{-/-}$ mice. (**D**) Mean percentage overlap values in wildtype and *Casp3*$^{-/-}$ mice and p-values of two-tailed t-tests between the two genotypes are listed for each cutoff threshold.

S9D), and fiber fraction (Fig. S9E) (46) in *Casp3*$^{+/+}$ and *Casp3*$^{-/-}$ mice. We found no significant difference between the two groups of animals, suggesting that the defective circuit refinement in *Casp3*$^{-/-}$ animals was not due to the lack of retinogeniculate synapse maturation but instead an inability to eliminate weak synapses.

An increased number of RGC inputs innervating dLGN relay neurons in *Casp3*$^{-/-}$ mice should correspond to greater numbers of presynaptic release sites and should result in more frequent spontaneous release of neurotransmitters. To test this prediction, we measured miniature EPSCs (mEPSCs) in dLGN relay neurons of *Casp3*$^{+/+}$ and *Casp3*$^{-/-}$ mice (**Fig. 4D**). We found that mEPSCs in *Casp3*$^{-/-}$ neurons occurred more frequently (**Fig. 4E**), with a greater fraction of them having small amplitudes (**Fig. 4F**). These results mirror previous measurements in hippocampal CA1 neurons in Casp3$^{-/-}$ mice (24). Overall, our observations are consistent with the model where caspase-3 deficiency impairs the removal of weak synapses, leading to greater number of inputs on dLGN relay neurons.

As an additional way to probe retinogeniculate circuit refinement, we measured paired-pulse response ratios (PPRs) in dLGN relay neurons (Fig. S8B and **Fig. 4G-H**) (45, 47). The retinogeniculate circuit typically generates PPRs that are smaller than one due to depletion of neurotransmitters (Fig. S8B) (45, 47). If there is an increase in the number of release sites in *Casp3*$^{-/-}$ mice, we expect more available neurotransmitters and larger PPRs (Fig. S8C) (47). Indeed, we observed higher PPRs in *Casp3*$^{-/-}$ dLGN relay neurons (**Fig. 4D-E**), suggesting that defective synapse elimination resulted in more RGC release sites in *Casp3*$^{-/-}$ mice. Taken together, our results demonstrate that caspase-3 is required for experience-driven retinogeniculate circuit refinement.

Caspase-3 deficiency impairs synapse elimination by microglia

Our results demonstrate that proper synapse elimination in the retinogeniculate pathway requires caspase-3 activity. Previous studies have shown that microglia and astrocytes engulf weak synapses during the process of synapse elimination (7, 10). We therefore sought to determine whether caspase-3 activation is required for synapse elimination by microglia and/or astrocytes.

If synapse elimination by microglia depends on caspase-3 activation, then microglia in *Casp3*$^{-/-}$ mice should engulf less synaptic material. Similar to a previous study (7), we utilized the *Cx3cr1-Gfp* transgenic mouse line to visualize microglia *in vivo.* In this line, the native *Cx3cr1* promoter drives *Gfp* expression and specifically labels microglia in the brain (**Fig. 5A**) (48). We labeled RGC axon terminals by injecting fluorophore-conjugated CTB in the eyes of P4 *Casp3*$^{+/-}$; *Cx3cr1-Gfp*$^{+/-}$ and *Casp3*$^{-/-}$; *Cx3cr1-Gfp*$^{+/-}$ littermate pups (*Casp3*$^{+/-}$ instead of *Casp3*$^{+/+}$ mice were used to enable more efficient breeding) (7). At P5, the brains were harvested and the dLGN imaged (**Figure 5A**). Microglia in *Casp3*$^{-/-}$; *Cx3cr1-Gfp*$^{+/-}$ mice had small soma and thin processes, indicating that caspase-3 deficiency did not result in microglial activation (**Fig. 5B**). This is further validated by immunohistochemical analysis of microglia in caspase-3 deficient mice (Fig. S10A-D). To quantify synapse engulfment, we isolated volumes corresponding to microglia and RGC axon terminals in the dLGN (**Fig. 5B**) and calculated the volume of RGC terminals that were fully enclosed in each microglia (**Fig. 5C**). As expected, we observed that microglia in *Casp3*$^{-/-}$; *Cx3cr1-Gfp*$^{+/-}$ mice engulfed significantly less axonal material compared to those of *Casp3*$^{+/-}$; *Cx3cr1-Gfp*$^{+/-}$ littermates (**Fig. 5B-C**). The same trend was observed when RGC axon terminals originating from the two eyes were analyzed separately (Fig. S11A-B). As the engulfment capacity of microglia is limited by their size, we normalized the volume of engulfed synaptic material in each microglia to the microglial volume (**Fig. 5D**). Microglia in both groups of mice are comparable in size (Fig. S11C), and the defective synaptic engulfment in *Casp3*$^{-/-}$ mice persisted after normalization to microglial volume (**Fig. 5D**). Additionally, the same defect was observed when engulfment values were averaged and reported by animal (Fig. S11D). Taken together, our results demonstrate that microglia-mediated synapse elimination depends on caspase-3.

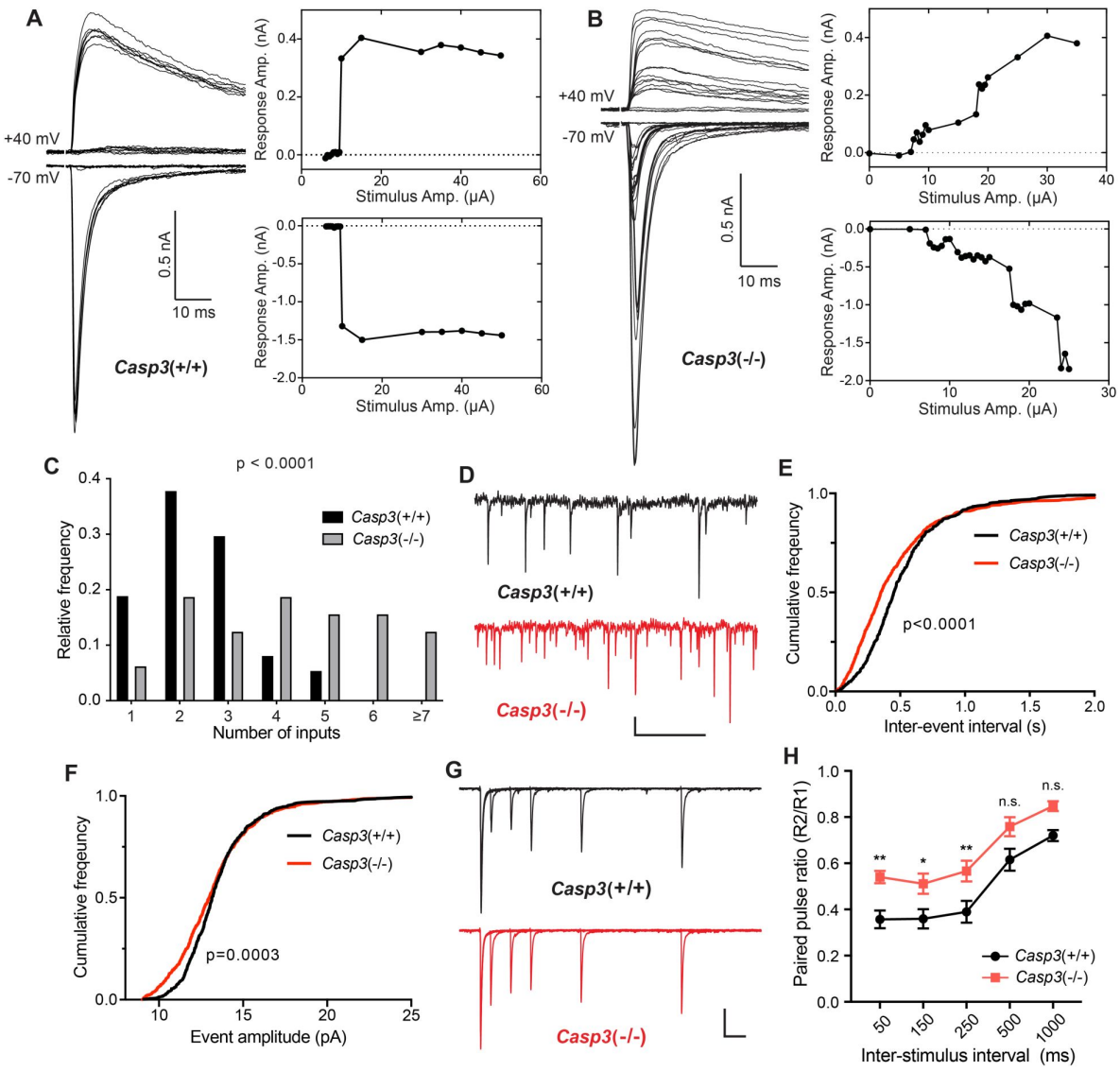

Figure 4.

Caspase 3 is required for retinogeniculate circuit refinement.

(**A**-**B**) Example recordings of dLGN relay neuron responses in P30 wildtype (**A**) and *Casp3*$^{-/-}$ (**B**) mice. Excitatory postsynaptic currents (EPSCs) were evoked by increasing stimulation currents in the optic tract. Both AMPAR-mediated inward current at -70 mV membrane potential and AMPAR and NMDAR-mediated outward current at +40 mV membrane potential are shown. Peak response amplitudes at each stimulation intensity are plotted to the right of recording traces. Scale bars represent 0.5 nA and 10 ms. (**C**) Distribution of RGC input numbers on individual dLGN relay neurons in wildtype and *Casp3*$^{-/-}$ mice. The number of RGC inputs was inferred by manually counting the number of steps in AMPAR-mediated EPSC response curves (lower right in **A** and **B**) while blind to the genotypes. P-value was calculated from two-tailed t-test. n=37 cells from 22 wildtype mice and n=32 cells from 16 *Casp3*$^{-/-}$ mice. (**D**) Example recordings of mEPSC measurements from wildtype and *Casp3*$^{-/-}$ mice. Scale-bars represent 0.5 s (horizontal) and 5 pA (vertical). (**E**-**F**) Cumulative distribution curves of inter-mEPSC intervals (**E**) and mEPSC amplitudes (**F**) in wildtype and *Casp3*$^{-/-}$ mice. P-values were calculated from Kolmogorov-Smirnov tests. n=16 cells from 4 wildtype mice and n=17 cells from 4 *Casp3*$^{-/-}$ mice. (**G**) Example recordings from paired pulse measurements at -70 mV membrane potential in wildtype and *Casp3*$^{-/-}$ mice. Traces from experiments with 50, 150, 250, 500, and 1000 ms inter-stimulus intervals are overlayed. Stimulus artifacts were removed from the traces for clarity. Scale-bars represent 100 ms (horizontal) and 0.3 nA (vertical). (**H**) Paired-pulse ratio (calculated as amplitude of the second response over that of the first response) in wildtype and *Casp3*$^{-/-}$ mice at various inter-stimulus intervals. Mean and standard error of the mean (SEM) are shown. P-values were calculated from Bonferroni's multiple comparison test. p=0.0067 for 50 ms interval, p=0.0369 for 150 ms interval, and p=0.0097 for 250 ms interval. n=16 cells from 7 wildtype mice and n=13 cells from 4 *Casp3*$^{-/-}$ mice.

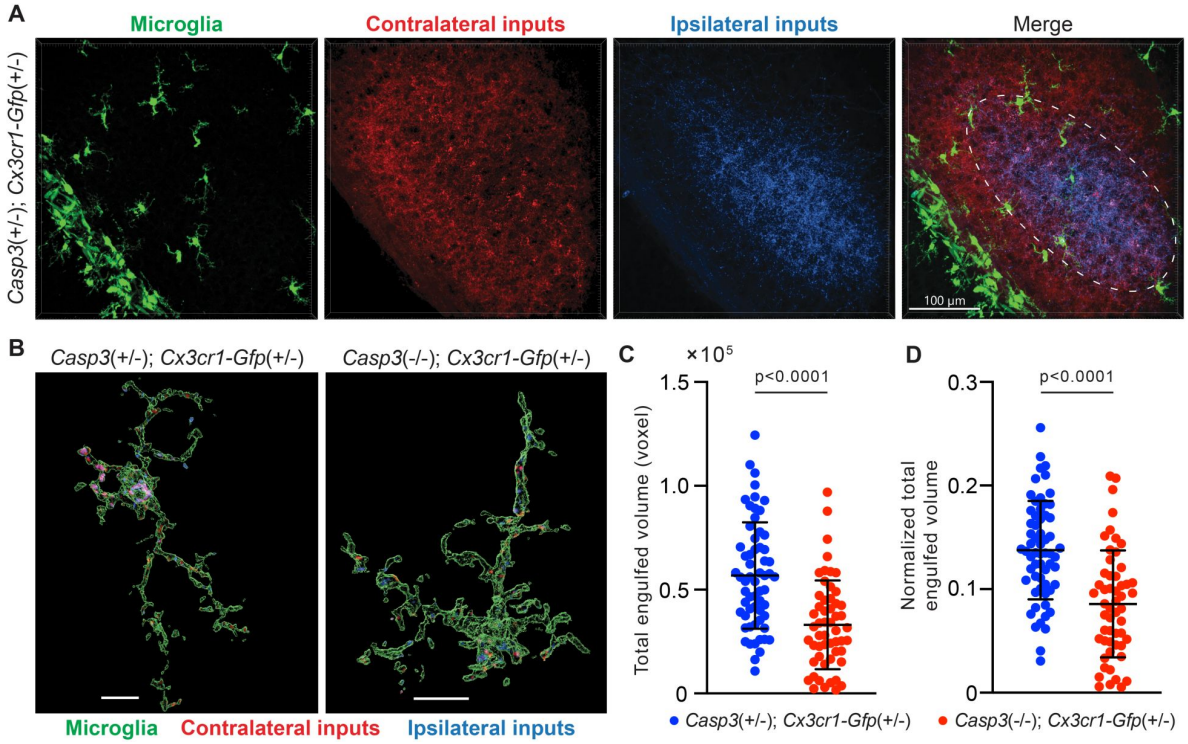

Figure 5.

Microglia-mediated synapse elimination depends on caspase-3.

(**A**) Representative 3D-reconstructed images of a P5 *Casp3*$^{+/-}$; *Cx3cr1-Gfp*$^{+/-}$ mouse dLGN with microglia displayed in green, contralateral RGC axon terminals in red, and ipsilateral RGC terminals in blue. In the merged image, the region from which microglia are selected for analysis is indicated with the dashed line. The scale-bar represents 100 µm. (**B**) Representative surface rendering of microglia (green) from P5 dLGNs of *Casp3*$^{+/-}$; *Cx3cr1-Gfp*$^{+/-}$ and *Casp3*$^{-/-}$; *Cx3cr1-Gfp*$^{+/-}$ mice. Intracellular contralateral (red) and ipsilateral (blue) RGC axon terminals are shown. Microglia from caspase-3 deficient mice engulf visibly less synaptic material. Scale-bars represent 10 µm. (**C**) Total volume of engulfed synaptic material in individual microglia from *Casp3*$^{+/-}$; *Cx3cr1-Gfp*$^{+/-}$ and *Casp3*$^{-/-}$; *Cx3cr1-Gfp*$^{+/-}$ mice. (**D**) Total volume of engulfed synaptic material in each microglia (from **C**) is normalized to the volume of that microglia. In **C**-**D**, each point represents one microglia. Mean and S.D. are shown. p-values were calculated from unpaired two-tailed t-tests. n=61 microglia from 8 *Casp3*$^{+/-}$; *Cx3cr1-Gfp*$^{+/-}$ mice and n=54 microglia from 5 *Casp3*$^{-/-}$; *Cx3cr1-Gfp*$^{+/-}$ mice.

To test whether caspase-3 activation is also required for astrocyte-mediated synapse elimination, we used the *Aldh1l1-Gfp* transgenic mouse line, where *Gfp* expression specifically labels astrocytes (Fig. S12A) (49). We again labeled RGC axon terminals in *Casp3*$^{+/-}$; *Aldh1l1-Gfp*$^{+/-}$ and *Casp3*$^{-/-}$; *Aldh1l1-Gfp*$^{+/-}$ littermate mice with CTB conjugates (Fig. S12A). Astrocytes were present in the P5 dLGN at a much higher density than microglia and possess very fine processes (Fig. S12A). To ensure segmentation fidelity, we only analyzed astrocyte cell bodies and their proximal processes (Fig. S12B). Unexpectedly, we found that the volume of axonal material engulfed by astrocytes was comparable in the two groups of mice (Fig. S12C). The same trend was observed when we normalized the volume of engulfed synaptic material to astrocyte volume (Fig. S12D-E). It is possible that, by using *Casp3*$^{+/-}$ mice instead of *Casp3*$^{+/+}$ mice as controls, we have obscured some defects in astrocyte-mediated synapse elimination. Nevertheless, given that astrocyte-mediated synapse elimination did not show clear dependence on caspase-3, we focused on measuring synapse engulfment by microglia as a readout of preferential elimination of weak synapses.

Removal of weak synapses by microglia requires caspase-3 activity

If caspase-3 activation at weak synapses is important for synapse removal, then in caspase-3 deficient mice, microglia should lose the ability to engulf weak synapses. To test this hypothesis, we inactivated retinogeniculate synapses originating from right eyes in *Casp3*$^{+/+}$ and *Casp3*$^{-/-}$ mice with AAV-hSyn-TeTxLC injections (**Fig. 6A**). A group of animals was included for each genotype that received control injections. To measure synapse engulfment by microglia, we labeled RGC axon terminals with CTB conjugates and visualized microglia by immunostaining against Iba1, a marker specific for microglia in the brain (**Fig. 6B-G**). According to our model, in TeTxLC-injected *Casp3*$^{+/+}$ mice, microglia should preferentially engulf inactive retinogeniculate synapses originating from the right eye (**Fig. 6A**), whereas in TeTxLC-injected *Casp3*$^{-/-}$ mice, synapses from the right and the left eye should be engulfed at similar levels regardless of their strength (**Fig. 6A**).

To quantitatively detect engulfment of weak synapses by microglia, we compared TeTxLC-injected and control-injected animals of the same genotype (**Fig. 6B, C**, and **F**). We first calculated the ratio between the volume of right eye-originated RGC axon terminals and left eye-originated terminals that were engulfed by each microglia. Then, by comparing this right-to-left engulfment ratio in TeTxLC-injected vs. control-injected animals, engulfment of inactive synapses could be detected as higher engulfment ratios in TeTxLC-injected animals (**Fig. 6F**). It is worth noting confounding factors, such as surgical manipulations, cancel out when calculating engulfment ratios, allowing information pertaining only to substrate preference to be isolated.

Consistent with previous studies (7), in *Casp3*$^{+/+}$ mice inactivation of retinogeniculate synapses from the right eye led to enhanced microglia-mediated engulfment of right eye-originated RGC axon terminals but not left eye-originated terminals (Fig. S13A-B), resulting in a significant increase in right-to-left engulfment ratios in microglia of TeTxLC-injected animals compared to control-injected animals (**Fig. 6B, C**, and **F**). In contrast, engulfment ratios were similar between TeTxLC-injected and control-injected *Casp3*$^{-/-}$ mice (**Fig. 6D, E** and **G** and Fig. S13C-D), suggesting that microglia could no longer distinguish between strong and weak synapses in the absence of caspase-3 activation. These observations remain valid when data were averaged and reported by animal (Fig. S13E-F). Summing the evidence obtained thus far, we propose the activity-dependent caspase-3 activation is a crucial signaling event that integrates upstream information about synaptic activity, takes place at weak/inactive synapses, and leads to activity-dependent elimination of weak synapses by microglia.

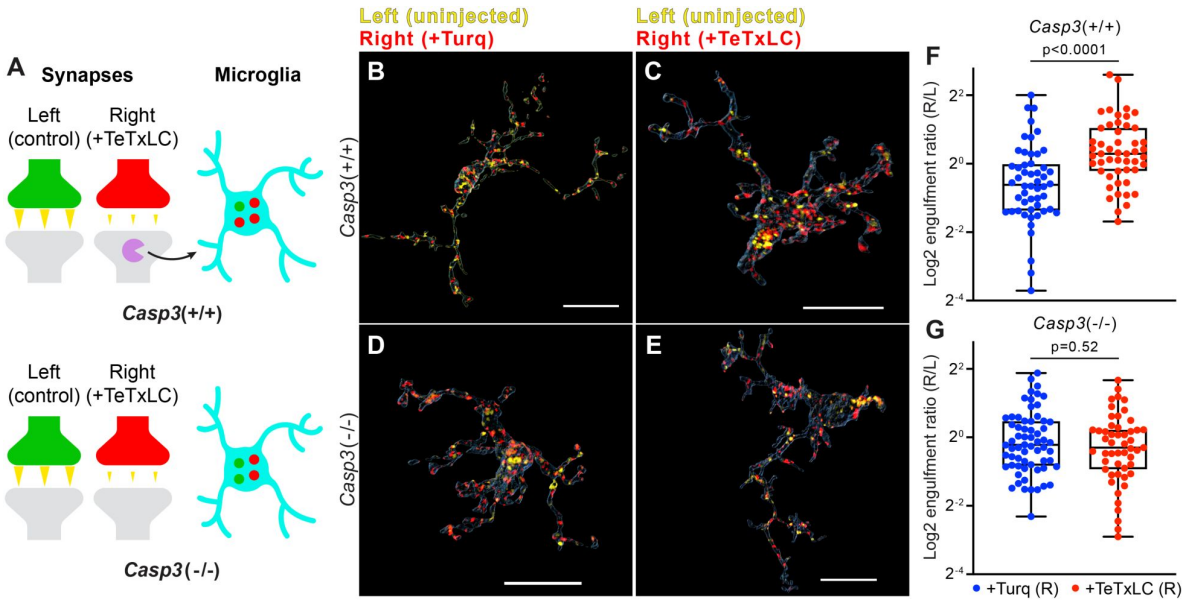

Figure 6.

Removal of weak synapses by microglia requires caspase-3 activity.

(**A**) Schematics illustrating the experimental rationale. In wildtype mice (upper panel), inactivating retinogeniculate synapses from the right eye activates caspase-3 (magenta) and recruits microglia to preferentially engulf right eye-originated synapses (red) over left eye-originated synapses (green). If caspase-3 activation is blocked (lower panel), engulfment of inactive synapses should be attenuated. (**B**-**E**) Surface rendering of representative microglia from P5 left dLGN of *Casp3*$^{+/+}$ (**B**-**C**) or *Casp3*$^{-/-}$ (**D**-**E**) mice injected with AAV that provided mTurquoise2 (**B** and **D**) or TeTxLC (**C** and **E**) in the right eye at E15. Microglia were labeled by immunostaining against Iba1. RGC axon terminals from the left eye are shown in yellow and terminals from the right eye in red. Scale bars represent 15 µm. (**F**-**G**) Ratio between volumes of right-eye and left-eye-originated synaptic material engulfed by microglia from *Casp3*$^{+/+}$ (**F**) or *Casp3*$^{-/-}$ (**G**) mice injected with AAV that carried the gene for mTurquoise2 (blue) or TeTxLC (red). Each dot represents one microglia. Engulfment ratios are displayed on a log scale. 0, 25, 50, 75, and 100 percentiles are shown. p-values were calculated from unpaired two-tailed Mann-Whitney tests. n=52 microglia from 7 Turq-injected *Casp3*$^{+/+}$ mice, n=50 microglia from 8 TeTxLC-injected *Casp3*$^{+/+}$ mice, n=64 microglia from 5 Turq-injected *Casp3*$^{-/-}$ mice, and n=51 microglia from 6 TeTxLC-injected *Casp3*$^{-/-}$ mice.

Caspase-3 deficiency protects against amyloid-β-induced synapse loss

Lastly, we wanted to test if caspase-3 regulates synapse loss in neurodegenerative diseases through mechanisms analogous to its role in activity-dependent synapse elimination. To this end, we focused on Alzheimer's disease (AD). AD is the most common cause of dementia (50), and synapse loss is the strongest correlate of cognitive decline in AD patients (51). Accumulation and deposition of oligomeric or fibril amyloid-β (Aβ) peptide has been proposed to be the cause of neurodegeneration in AD (50). Intriguingly, oligomeric Aβ impairs long-term potentiation (LTP) (52), and this suppression of LTP requires caspase-3 activation (53). Additionally, caspase-3 activation has been linked to early synaptic dysfunction in an AD mouse model (54).

To test if synapse loss in AD is regulated by caspase-3, we utilized the APP/PS1 mouse line, in which amyloid precursor protein (APP) and presenilin 1 (PS1) carrying mutations associated with early-onset familial AD are overexpressed in CNS neurons (55). We observed that female *App/Ps1*$^{+/-}$ mice developed amyloid deposits in the hippocampus and cortex by 5 months (Fig. S14Aii), and that the amyloid burden worsened by 6 months (Fig. S14Aiii). In male *App/Ps1*$^{+/-}$ mice, amyloid deposits only became apparent at 6 months and occurred at a lower level compared to age-matched females (Fig. S14Aiv-v). We focused on analyzing *App/Ps1*$^{+/-}$ female mice in subsequent experiments to obtain robust phenotypes. To quantify synapse loss, we labeled presynaptic and postsynaptic compartments in the dentate gyrus of 6 month-old *App/Ps1*$^{-/-}$ and *App/Ps1*$^{+/-}$ littermates by detecting synaptic vesicle protein 2 (SV2) and Homer1, respectively, and selected multiple fields of interest per animal for imaging analysis while avoiding regions adjacent to amyloid deposits (Fig. S15). We fitted ellipsoids to SV2 and Homer1 signals to identify pre- and post-synaptic puncta and defined synapses as Homer1-SV2 puncta pairs that were less than 300 nm apart (**Fig. 7A**). We observed that synapse density in *App/Ps1*$^{+/-}$ mice was significantly reduced compared to that in *App/Ps1*$^{-/-}$ littermate controls (**Fig. 7A-B**), and that this reduction could be attributed to lower densities of both pre- and post-synaptic puncta in *App/Ps1*$^{+/-}$ mice (Fig. S16A-B). We then crossed APP/PS1 mice to caspase-3 deficient mice and quantified synapse density in 6 month-old *Casp3*$^{-/-}$; *App/Ps1*$^{-/-}$ and *Casp3*$^{-/-}$; *App/Ps1*$^{+/-}$ littermate mice (Fig. S15). We observed that, in the caspase-3 deficient background, overexpression of mutant APP and PS1 no longer resulted in a reduction in the density of synapses (**Fig. 7C-D**) or pre-/post-synaptic puncta (Fig. S16C-D), suggesting that caspase-3 activity is required for Aβ-induced synapse loss in the APP/PS1 mouse model. Intriguingly, levels of amyloid deposition were comparable between *App/Ps1*$^{+/-}$ and *Casp3*$^{-/-}$; *App/Ps1*$^{+/-}$ mice (Fig. S14Avi and B), and reactive microglia were observed near amyloid deposits regardless of caspase-3 deficiency (Fig. S17), indicating that protection conferred by caspase-3 deficiency against Aβ-induced synapse loss might not require inhibition of amyloid accumulation or microgliosis. We also investigated whether Aβ accumulation induced elevated levels of caspase-3 activity. We analyzed 4, 5, and 6 month-old *App/Ps1*$^{-/-}$ and *App/Ps1*$^{+/-}$ mice but only observed robust upregulation of caspase-3 activity in the dentate gyrus of a subset of 4 month-old *App/Ps1*$^{+/-}$ mice (Fig. S18A-C). Upregulated caspase-3 activity in these mice remained in a punctate pattern without inducing neuronal death (Fig. S18D-F). It is possible that Aβ transiently induces caspase-3 activation in *App/Ps1*$^{+/-}$ mice, but stochasticity in the onset and duration of such induction prevents reliable detection with our sample size and temporal resolution. Overall, our results demonstrate caspase-3 as an important regulator of Aβ-induced synapse loss and a potential therapeutic target for AD treatment.

Discussion

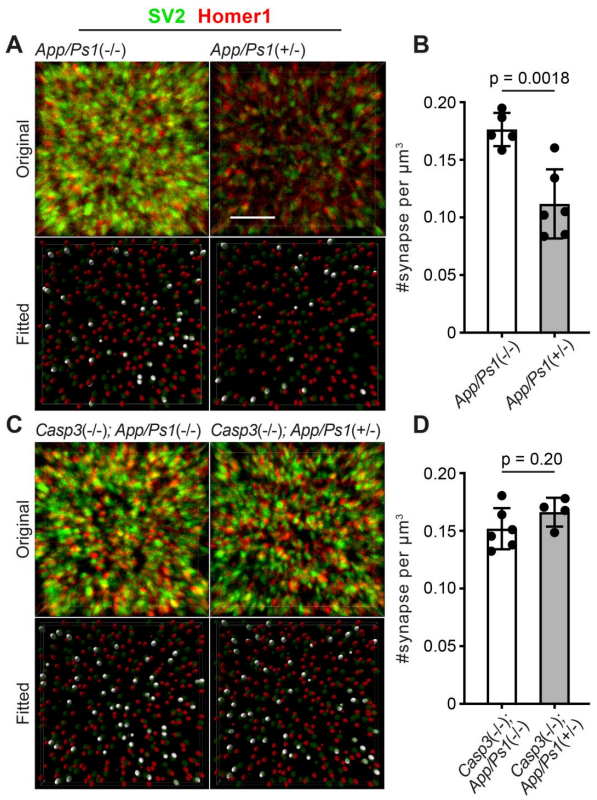

Figure 7.

Caspase-3 deficiency protects against Aβ induced synapse loss.

(**A** and **C**) Representative 3D-reconstructed images (3 µm in z) showing presynaptic (SV2, in green) and postsynaptic (Homer1, in red) signals in dentate gyrus of female 6 month-old APP/PS1 mice on caspase-3 wildtype (**A**) and deficient (**C**) backgrounds. Ellipsoids were fitted to the original images (upper panels) to isolate pre-(green) and post-synaptic (red) puncta (lower panels). Homer1 ellipsoids found with 300 nm of a SV2 ellipsoid are highlighted in white in the fitted images. Original images are adjusted to the same contrast. For the fitted images, only ellipsoids from the upper half of the z-stack are shown. Scale-bar represents 4 µm. (**B** and **D**) Quantification of synapse density in APP/PS1 mice on caspase-3 wildtype (**B**) and deficient (**D**) backgrounds. Mean and S.D. are shown. p-values were calculated from unpaired two-tailed t-tests. n=5 for *App/Ps1*$^{-/-}$ mice, n=6 for *App/Ps1*$^{+/-}$ mice, n=6 for *Casp3*$^{-/-}$; *App/Ps1*$^{-/-}$ mice, and n=4 for *Casp3*$^{-/-}$; *App/Ps1*$^{+/-}$ mice.

A model for caspase-3 dependent synapse elimination

Our findings support a model where competitive interaction between strong synapses and weak synapses in the retinogeniculate pathway triggers caspase-3 activation in the postsynaptic compartments of weak synapses. Caspase-3 activation results in the removal of weaker synaptic connections by microglia, thereby facilitating the establishment of mature circuits in the visual pathway.

Mechanisms of activity-dependent caspase-3 activation

In the experiment where we demonstrated activity-dependent caspase-3 activation, we inactivated all retinogeniculate synapses from one eye to induce sufficiently high caspase-3 activity that can be discerned from background. Widespread caspase-3 activity induced by such strong inactivation at multiple sites in a given cell likely self-amplifies through positive feedback (35) and overwhelms negative regulation mechanisms (e.g., ubiquitin-dependent proteasomal degradation (24, 33, 34)), leading to the observed apoptosis of entire dLGN relay neurons (**Fig. 1B**). However, apoptotic neurons were infrequently observed in the dLGN of control animals (**Fig. 1D** and **2B**), and caspase-3 deficiency does not significantly alter dLGN relay neuron numbers (Fig. S7), suggesting that during normal development, activity-dependent caspase-3 activation is predominantly localized and generally does not lead to neuronal death.

Intriguingly, synaptic inactivation in our experiment was achieved through TeTxLC expression in presynaptic RGCs, but caspase-3 activation was observed in postsynaptic relay neurons. Conversely, while caspase-3 is activated in the postsynaptic compartment, we were able to detect defects in synapse elimination using assays that measure presynaptic inputs. These observations suggest that activity-dependent caspase-3 activation requires synaptic transmission, and that caspase-3 dependent synapse elimination is not strictly axonal or dendritic but involves both pre- and post-synaptic compartments. An important limitation of this study is that experiments in full-body *Casp3*$^{-/-}$ mice cannot query the roles of caspase-3 in presynaptic and postsynaptic compartments separately. Future experiments that perturb caspase-3 activation and other signaling events specifically in the pre- or post-synaptic compartments are needed to reveal more detailed mechanisms of activity-dependent synapse elimination.

The observation that activity-dependent caspase-3 activation requires the presence of both weak and strong synapses resonates with previous research demonstrating that relative synaptic efficacy biases the outcome of synapse elimination during development of neuromuscular junctions and the callosal pathway (15, 36, 56, 57). However, the mechanisms linking synaptic competition with caspase-3 activation remains elusive. During LTD, caspase-3 is activated through mitochondrial release of cytochrome-c (18). Whether synaptic competition could induce caspase-3 activation via mechanisms such as calcium signaling, which regulates both neurotransmission and cytochrome-c release (58), is an outstanding question.

Link between caspase-3 activation and synapse engulfment by microglia

How does caspase-3 activation at weak synapses lead to synapse engulfment by microglia? Caspase-3 activation is known to trigger the display of apoptosis markers that can be recognized by phagocytes (19). One of the best understood markers is phosphatidylserine (PtdSer), a phospholipid that translocates from the cytoplasmic leaflet of the plasma membrane to the exoplasmic leaflet during apoptosis (19). Importantly, caspase-3 directly regulates the enzymes that translocate PtdSer through enzymatic cleavage (59, 60). Two recent studies demonstrated that PtdSer is displayed on retinogeniculate synapses during postnatal development,

and microglia use the exposed PtdSer as a cue to target and engulf synapses (8, 9). Whether PtdSer exposure is upregulated in response to synapse weakening and whether caspase-3 activity is required for such exposure are important questions that require further investigation.

The complement protein C1q has been observed to bind to PtdSer on apoptotic cells and facilitate phagocytic clearance (19). Additionally, a previous study found caspase-3 activity in C1q-positive synaptosomes (61), suggesting that C1q may bridge caspase-3 activation and synapse elimination. However, we investigated C1q expression and localization in the dLGN of P5 TeTxLC-injected mice but did not observe upregulation of C1q abundance or colocalization between C1q and caspase-3 activity (data not shown). It is often assumed in the literature that microglia directly engulf intact synapses, but existing data also support an alternative model where microglia indirectly contribute to synapse elimination by engulfing synaptic debris that is shed through neuron-autonomous mechanisms (62). The observation that synaptic activity promotes microglial engulfment through caspase-3 activation raises the possibility that weakened synapses partially disintegrate through apoptosis-like mechanisms prior to being engulfed by microglia. Further studies are needed to elucidate the intermediate steps between caspase-3 activation and microglial engulfment of synapses.

Caspase-3 as a potential target for AD treatment

Our findings suggest that caspase-3 deficiency confers protection against Aβ-induced synapse loss in a mouse model of AD. Notably, the absence of caspase-3 does not seem to affect Aβ deposition or microglia reactivity, indicating that caspase-3 depletion may mitigate synapse loss by directly countering Aβ-induced synaptic toxicity. Given the prominence of Aβ and inflammation as targets for AD drug development (63), inhibiting caspase-3 activity offers a potential alternative therapeutic strategy that could complement and enhance current treatment approaches. Therefore, it is important to test whether pharmacological inhibition of caspase-3 can effectively slow synapse loss and cognitive decline in both mouse models of AD and human patients.

Acknowledgements

We thank Crystall Lopez, Benjamin Gantz, and Brooke Groff for help with animal husbandry and breeding. We thank Sarah Lindo, Colin Morrow, Claire Boyer, and Rae Demars for help with surgery. We thank Monique Copeland, Amy Hu, Morgan Clarke, and Benjamin Foster for help with histology. We are also grateful to Sarah Kivimaki and the Viral Tools team of Janelia Core Services for help with AAV preparation. We thank Dr. Cagla Eroglu, Dr. Richard Axel, and Dr. David Clapham for comments on the manuscript. This work is supported by the Howard Hughes Medical Institute.

Additional files

Supplementary figures

Methods

References

1. Kano M., Hashimoto K. 2009) **Synapse elimination in the central nervous system** *Curr Opin Neurobiol* **19**:154–161

2. Faust T. E., Gunner G., Schafer D. P. 2021) **Mechanisms governing activity-dependent synaptic pruning in the developing mammalian CNS** *Nat Rev Neurosci* **22**:657–673

3. Riccomagno M. M., Kolodkin A. L. 2015) **Sculpting neural circuits by axon and dendrite pruning** *Annu Rev Cell Dev Biol* **31**:779–805

4. Katz L. C., Shatz C. J. 1996) **Synaptic activity and the construction of cortical circuits** *Science* **274**:1133–1138

5. Hua J. Y., Smith S. J. 2004) **Neural activity and the dynamics of central nervous system development** *Nat Neurosci* **7**:327–332

6. Stevens B., et al. 2007) **The classical complement cascade mediates CNS synapse elimination** *Cell* **131**:1164–1178

7. Schafer D. P., et al. 2012) **Microglia sculpt postnatal neural circuits in an activity and complement-dependent manner** *Neuron* **74**:691–705

8. Li T., et al. 2020) **A splicing isoform of GPR56 mediates microglial synaptic refinement via phosphatidylserine binding** *Embo J* **39**:e104136

9. Scott-Hewitt N., et al. 2020) **Local externalization of phosphatidylserine mediates developmental synaptic pruning by microglia** *Embo J* **39**:e105380

10. Chung W. S., et al. 2013) **Astrocytes mediate synapse elimination through MEGF10 and MERTK pathways** *Nature* **504**:394–400

11. Wilton D. K., Dissing-Olesen L., Stevens B. 2019) **Neuron-Glia Signaling in Synapse Elimination** *Annu Rev Neurosci* **42**:107–127

12. Chung W. S., Allen N. J., Eroglu C. 2015) **Astrocytes Control Synapse Formation, Function, and Elimination** *Cold Spring Harb Perspect Biol* **7**:a020370

13. Li Q., Barres B. A. 2018) **Microglia and macrophages in brain homeostasis and disease** *Nat Rev Immunol* **18**:225–242

14. Paolicelli R. C., et al. 2011) **Synaptic pruning by microglia is necessary for normal brain development** *Science* **333**:1456–1458

15. Yasuda M., Nagappan-Chettiar S., Johnson-Venkatesh E. M., Umemori H. 2021) **An activity-dependent determinant of synapse elimination in the mammalian brain** *Neuron* **109**:1333–1349

16. Philips R. L., et al. 2022) **The JAK-STAT pathway at 30: Much learned, much more to do** *Cell* **185**:3857–3876

17. McIlwain D. R., Berger T., Mak T. W. 2013) **Caspase functions in cell death and disease** *Cold Spring Harb Perspect Biol* **5**

18. Li Z., et al. 2010) **Caspase-3 Activation via Mitochondria Is Required for Long-Term Depression and AMPA Receptor Internalization** *Cell* **141**:859–871

19. Park S. Y., Kim I. S. 2017) **Engulfment signals and the phagocytic machinery for apoptotic cell clearance** *Exp Mol Med* **49**

20. Trouw L. A., Blom A. M., Gasque P. 2008) **Role of complement and complement regulators in the removal of apoptotic cells** *Mol Immunol* **45**:1199–1207

21. Williams D. W., Kondo S., Krzyzanowska A., Hiromi Y., Truman J. W. 2006) **Local caspase activity directs engulfment of dendrites during pruning** *Nat Neurosci* **9**:1234–1236

22. Kuo C. T., Zhu S., Younger S., Jan L. Y., Jan Y. N. 2006) **Identification of E2/E3 ubiquitinating enzymes and caspase activity regulating Drosophila sensory neuron dendrite pruning** *Neuron* **51**:283–290

23. Simon D. J., et al. 2012) **A caspase cascade regulating developmental axon degeneration** *J Neurosci* **32**:17540–17553

24. Erturk A., Wang Y., Sheng M. 2014) **Local pruning of dendrites and spines by caspase-3-dependent and proteasome-limited mechanisms** *J Neurosci* **34**:1672–1688

25. Liang L., Chen C. 2020) **Organization, Function, and Development of the Mouse Retinogeniculate Synapse** *Annu Rev Vis Sci* **6**:261–285

26. Penn A. A., Riquelme P. A., Feller M. B., Shatz C. J. 1998) **Competition in retinogeniculate patterning driven by spontaneous activity** *Science* **279**:2108–2112

27. Stellwagen D., Shatz C. J. 2002) **An instructive role for retinal waves in the development of retinogeniculate connectivity** *Neuron* **33**:357–367

28. Yasuda M., Nagappan-Chettiar S., Umemori H. 2021) **In utero intraocular AAV injection for early gene expression in the developing rodent retina** *STAR Protoc* **2**:100742

29. Schiavo G., et al. 1992) **Tetanus and botulinum-B neurotoxins block neurotransmitter release by proteolytic cleavage of synaptobrevin** *Nature* **359**:832–835

30. Torborg C. L., Feller M. B. 2004) **Unbiased analysis of bulk axonal segregation patterns** *J Neurosci Meth* **135**:17–26

31. Krahe T. E., El-Danaf R. N., Dilger E. K., Henderson S. C., Guido W. 2011) **Morphologically distinct classes of relay cells exhibit regional preferences in the dorsal lateral geniculate nucleus of the mouse** *J Neurosci* **31**:17437–17448

32. Parnavelas J. G., Mounty E. J., Bradford R., Lieberman A. R. 1977) **The postnatal development of neurons in the dorsal lateral geniculate nucleus of the rat: a Golgi study** *J Comp Neurol* **171**:481–499

33. Choi Y. E., et al. 2009) **The E3 ubiquitin ligase cIAP1 binds and ubiquitinates caspase-3 and -7 via unique mechanisms at distinct steps in their processing** *J Biol Chem* **284**:12772–12782

34. Suzuki Y., Nakabayashi Y., Takahashi R. 2001) **Ubiquitin-protein ligase activity of X-linked inhibitor of apoptosis protein promotes proteasomal degradation of caspase-3 and enhances its anti-apoptotic effect in Fas-induced cell death** *Proc Natl Acad Sci U S A* **98**:8662–8667

35. McComb S., et al. 2019) **Efficient apoptosis requires feedback amplification of upstream apoptotic signals by effector caspase-3 or -7** *Sci Adv* **5**:eaau9433

36. Nagappan-Chettiar S., Yasuda M., Johnson-Venkatesh E. M., Umemori H. 2023) **The molecular signals that regulate activity-dependent synapse refinement in the brain** *Curr Opin Neurobiol* **79**:102692

37. Rossi F. M., et al. 2001) **Requirement of the nicotinic acetylcholine receptor beta 2 subunit for the anatomical and functional development of the visual system** *Proc Natl Acad Sci U S A* **98**:6453–6458

38. Kuida K., et al. 1996) **Decreased apoptosis in the brain and premature lethality in CPP32-deficient mice** *Nature* **384**:368–372

39. Houde C., et al. 2004) **Caspase-7 expanded function and intrinsic expression level underlies strain-specific brain phenotype of caspase-3-null mice** *J Neurosci* **24**:9977–9984

40. De Haan L., Hirst T. R. 2004) **Cholera toxin: a paradigm for multi-functional engagement of cellular mechanisms (Review)** *Mol Membr Biol* **21**:77–92

41. Otsu N. 1979) **A Threshold Selection Method from Gray-Level Histograms** *IEEE Transactions on Systems, Man, and Cybernetics* **9**:62–66

42. Young R. W. 1984) **Cell death during differentiation of the retina in the mouse** *J Comp Neurol* **229**:362–373

43. Dreher B., Potts R. A., Bennett M. R. 1983) **Evidence that the early postnatal reduction in the number of rat retinal ganglion cells is due to a wave of ganglion cell death** *Neurosci Lett* **36**:255–260

44. Rodriguez A. R., de Sevilla Muller L. P., Brecha N. C. 2014) **The RNA binding protein RBPMS is a selective marker of ganglion cells in the mammalian retina** *J Comp Neurol* **522**:1411–1443

45. Chen C., Regehr W. G. 2000) **Developmental remodeling of the retinogeniculate synapse** *Neuron* **28**:955–966

46. Hooks B. M., Chen C. 2006) **Distinct roles for spontaneous and visual activity in remodeling of the retinogeniculate synapse** *Neuron* **52**:281–291

47. Regehr W. G. 2012) **Short-term presynaptic plasticity** *Cold Spring Harb Perspect Biol* **4**:a005702

48. Jung S., et al. 2000) **Analysis of fractalkine receptor CX(3)CR1 function by targeted deletion and green fluorescent protein reporter gene insertion** *Mol Cell Biol* **20**:4106–4114

49. Gong S., et al. 2003) **A gene expression atlas of the central nervous system based on bacterial artificial chromosomes** *Nature* **425**:917–925

50. Knopman D. S., et al. 2021) **Alzheimer disease** *Nat Rev Dis Primers* **7**:33

51. Meftah S., Gan J. 2023) **Alzheimer's disease as a synaptopathy: Evidence for dysfunction of synapses during disease progression** *Front Synaptic Neurosci* **15**

52. Shankar G. M., et al. 2008) **Amyloid-beta protein dimers isolated directly from Alzheimer's brains impair synaptic plasticity and memory** *Nat Med* **14**:837–842

53. Jo J., et al. 2011) **Abeta(1-42) inhibition of LTP is mediated by a signaling pathway involving caspase-3, Akt1 and GSK-3beta** *Nat Neurosci* **14**:545–547

54. D'Amelio M., et al. 2011) **Caspase-3 triggers early synaptic dysfunction in a mouse model of Alzheimer's disease** *Nat Neurosci* **14**:69–76

55. Jankowsky J. L., et al. 2004) **Mutant presenilins specifically elevate the levels of the 42 residue beta-amyloid peptide in vivo: evidence for augmentation of a 42-specific gamma secretase** *Hum Mol Genet* **13**:159–170

56. Buffelli M., et al. 2003) **Genetic evidence that relative synaptic efficacy biases the outcome of synaptic competition** *Nature* **424**:430–434

57. Lee Y. I. 2020) **Developmental neuromuscular synapse elimination: Activity-dependence and potential downstream effector mechanisms** *Neurosci Lett* **718**:134724

58. Garrido C., et al. 2006) **Mechanisms of cytochrome c release from mitochondria** *Cell Death Differ* **13**:1423–1433

59. Suzuki J., Denning D. P., Imanishi E., Horvitz H. R., Nagata S. 2013) **Xk-Related Protein 8 and CED-8 Promote Phosphatidylserine Exposure in Apoptotic Cells** *Science* **341**:403–406

60. Segawa K., et al. 2014) **Caspase-mediated cleavage of phospholipid flippase for apoptotic phosphatidylserine exposure** *Science* **344**:1164–1168

61. Gyorffy B. A., et al. 2018) **Local apoptotic-like mechanisms underlie complement-mediated synaptic pruning** *Proc Natl Acad Sci U S A* **115**:6303–6308

62. Eyo U., Molofsky A. V. 2023) **Defining microglial-synapse interactions** *Science* **381**:1155–1156

63. van Bokhoven P., et al. 2021) **The Alzheimer's disease drug development landscape** *Alzheimers Res Ther* **13**:186

Author information

Zhou Yu[†]
Janelia Research Campus, Howard Hughes Medical Institute, Ashburn, United States, Current address: Brigham and Women's Hospital, Harvard Medical School, Boston, United States
ORCID iD: 0000-0003-3213-4583

For correspondence: zyu3@bwh.harvard.edu
[†]These authors contributed equally.

Andrian Gutu[†]
Janelia Research Campus, Howard Hughes Medical Institute, Ashburn, United States

[†]These authors contributed equally.

Namsoo Kim
Janelia Research Campus, Howard Hughes Medical Institute, Ashburn, United States

Erin K O'Shea
Janelia Research Campus, Howard Hughes Medical Institute, Ashburn, United States
ORCID iD: 0000-0002-2649-1018

For correspondence: osheae@hhmi.org

Editors

Reviewer #2 (Public review):

This manuscript by Yu et al. demonstrates that activation of caspase-3 is essential for synapse elimination by microglia, but not by astrocytes. This study also reveals that caspase-3 activation-mediated synapse elimination is required for retinogeniculate circuit refinement and eye-specific territories segregation in dLGN in an activity-dependent manner. Inhibition of synaptic activity increases caspase-3 activation and microglial phagocytosis, while caspase-3 deficiency blocks microglia-mediated synapse elimination and circuit refinement in the dLGN. The authors further demonstrate that caspase-3 activation mediates synapse loss in AD, loss of caspase-3 prevented synapse loss in AD mice. Overall, this study reveals that caspase-3 activation is an important mechanism underlying the selectivity of microglia-mediated synapse elimination during brain development and in neurodegenerative diseases.

A previous study (Gyorffy B. et al., PNSA 2018) has shown that caspase-3 signal correlates with C1q tagging of synapses (mostly using in vitro approaches), which suggests that caspase-3 would be an underlying mechanism of microglial selection of synapses for removal. The current study provides convincing in vivo evidence demonstrating that caspase-3 activation is essential for microglial elimination of synapses during both brain development and neurodegeneration.

https://doi.org/10.7554/eLife.101779.2.sa1

Author response:

The following is the authors' response to the original reviews.

> ***Public Reviews:***
>
> ***Reviewer #1 (Public Review):***
>
> *In this manuscript, the authors study the effects of synaptic activity on the process of eye-specific segregation, focusing on the role of caspase 3, classically associated with apoptosis. The method for synaptic silencing is elegant and requires intrauterine injection of a tetanus toxin light chain into the eye. The authors report that this silencing leads to increased caspase 3 in the contralateral eye (Figure 1) and demonstrate evidence of punctate caspase 3 that does not overlap neuronal markers like map2. However, the quantifications showing increased caspase 3 in the silenced eye (done at P5) are complicated by overlap with the signal from entire dying cells in the thalamus. The authors also show that global caspase 3 deficiency impairs the process of eye-specific segregation and circuit refinement (Figures 3-4).*

The reviewer states: “this silencing leads to increased caspase 3 in the contralateral eye”. We observed increased caspase-3 activity, not protein levels, in the contralateral dLGN, not eye.

The reviewer states: “and demonstrate evidence of punctate caspase 3 that does not overlap neuronal markers like map2”. We do not believe that this statement is accurate, as we show that the punctate active caspase-3 signals overlap with the dendritic marker MAP2 (Figure S4A).

The reviewer also states: “, the quantifications showing increased caspase 3 [*activity*] in the silenced [*dLGN*] (done at P5) are complicated by overlap with the signal from entire dying cells in the thalamus”. We do not believe that this statement is accurate. The apoptotic neurons we observed are relay neurons (confirmed by their morphology and positive staining of NeuN – Figure S4B-C) located in the dLGN (the dLGN is clearly labeled by expression of fluorescent proteins in RGCs, and only caspase-3 activity in the dLGN area is analyzed), not “cells” of unknown lineage (as suggested by the reviewer) in the general “thalamus” area (as suggested by the reviewer). If the dying cells were non-neuronal cells, that would indeed confound our quantification and conclusions, but that is not the case.

We argue that whole-cell caspase-3 activation in dLGN relay neurons is a *bona fide* response to synaptic silencing by TeTxLC and therefore should be included in the quantification. We have two sets of controls: one is between the strongly inactivated dLGN and the weakly inactivated dLGN in the same TeTxLC-injected animal; and the second is between the dLGN of TeTxLC-injected animals and mock-injected animals. In both controls, only the dLGNs receiving strong synapse inactivation have more apoptotic dLGN relay neurons, demonstrating that these cells occur because of synapse inactivation. It is also unlikely that our perturbation is causing cell death through a non-synaptic mechanism. Since mock injections do not cause apoptosis in dLGN neurons, this phenomenon is not related to surgical damage. TeTxLC is injected into the eyes and only expressed in presynaptic RGCs, not in postsynaptic relay neurons, so this phenomenon is also unlikely to be caused by TeTxLC-related toxicity. Furthermore, if apoptosis of dLGN relay neurons is not related to synapse inactivation, then when TeTxLC is injected into both eyes, one would expect to see either the same amount or more apoptotic relay neurons, but we instead observed a reduction in dLGN neuron apoptosis, suggesting that synapse-related mechanisms are responsible. Considering the above, occasional whole-cell caspase-3 activation in relay neurons in TeTxLC-inactivated dLGN is causally linked to synapse inactivation and should be included in the quantification.

We also revised the manuscript to better explain the possible mechanistic connection between localized caspase-3 activity and whole-cell caspase-3 activity. We propose that whole-cell caspase-3 activation occurs because of uncontrolled accumulation of localized caspase-3 activation. Please see line 127-140 and line 403-413 for details.

Additionally, we would like to clarify that we are not claiming that synapse inactivation leads to only localized caspase-3 activation or only whole-cell caspase-3 activation, as is suggested by the editors and reviewers in the eLife assessment. We have clearly stated in the manuscript that both types of signals were observed. However, we reasoned that, because whole-cell caspase-3 activation in unperturbed dLGNs – which undergo normal synapse elimination – is infrequently observed, whole-cell caspase-3 activation may not be a significant driver of synapse elimination during normal development. In this revision, we included a new experiment to corroborate this hypothesis. If whole-cell caspase-3 activation in dLGN relay neurons is a prevalent phenomenon during normal development, such caspase-3 activity would lead to significant death of dLGN relay neurons during normal development. Consequently, if we block caspase-3 activation by deleting caspase-3, the number of relay neurons in the dLGN should increase. However, in support of our hypothesis, we observed comparable numbers of relay neurons in *Casp3*$^{+/+}$ and *Casp3*$^{-/-}$ mice. Please see Figure S7 for details.

> *The authors also report that "synapse weakening-induced caspase-3 activation determines the specificity of synapse elimination mediated by microglia but not astrocytes" (abstract). They report that microglia engulf fewer RGC axon terminals in caspase 3 deficient animals (Figure 5), and that this preferentially occurs in silenced terminals, but this preferential effect is lost in caspase 3 knockouts. Based on this, the authors conclude that caspase 3 directs microglia to eliminate weaker synapses. However, a much simpler and critical experiment that the authors did not perform is to eliminate microglia and show that the caspase 3 dependent effects go away. Without this experiment, there is no reason to assume that microglia are directing synaptic elimination.*

The reviewer states: “microglia engulf fewer RGC axon terminals in caspase 3 deficient animals (Figure 5), and that this preferentially occurs in silenced terminals, but this preferential effect is lost in caspase 3 knockouts”. We are not sure what the reviewer means by “this preferentially occurs in silenced terminals”. Our results show that microglia preferentially engulf silenced terminals, and such preference is lost in caspase-3 deficient mice (Figure 6).

We do not understand the experiment where the reviewer suggested to: “eliminate microglia and show that the caspase 3 dependent effects go away”. To quantify caspase-3 dependent engulfment of synaptic material by microglia or preferential engulfment of silenced terminals by microglia, microglia must be present in the tissue sample. If we eliminate microglia, neither of these measurements can be made. What could be measured if microglia are eliminated is the refinement of retinogeniculate pathway. This experiment would test whether microglia are required for caspase-3 dependent phenotypes. This is not a claim made in the manuscript. Instead, we claimed caspase-3 is required for microglia to engulf weak synapses, as supported by the evidence presented in Figure 6.

We did not claim that “microglia are directing synaptic elimination”. Our claim is that synapse inactivation induces caspase-3 activity, and caspase-3 activation in turn leads to engulfment of weak synapses by microglia. Based on this model, it is the neuronal activity that fundamentally directs synapse elimination. Synapse engulfment by microglia is only a readout we used to measure the outcome of activity-dependent synapse elimination. We have revised all sections in the manuscript that are related to synapse engulfment by microglia to emphasize the logic of this model.

We have also revised the abstract and title of the paper to better align it with our main claims, removed the reference to astrocytes, and clarified that microglia engulfment measurements are used as readouts of synapse elimination.

> *Finally, the authors also report that caspase 3 deficiency alters synapse loss in 6-month-old female APP/PS1 mice, but this is not really related to the rest of the paper.*

We respectfully disagree that Figure 7 is not related to the rest of the paper. Many genes involved in postnatal synapse elimination, such as C1q and C3, have been implicated in neurodegeneration. It is therefore natural and important to ask whether the function of caspase-3 in regulating synaptic homeostasis extends to neurodegenerative diseases in adult animals. The answer to this question may have broad therapeutic impacts.

> ***Reviewer #2 (Public Review):***
>
> *Summary:*
>
> *This manuscript by Yu et al. demonstrates that activation of caspase-3 is essential for synapse elimination by microglia, but not by astrocytes. This study also reveals that caspase 3 activation-mediated synapse elimination is required for retinogeniculate circuit refinement and eye-specific territories segregation in dLGN in an activity-dependent manner. Inhibition of synaptic activity increases caspase-3 activation and microglial phagocytosis, while caspase-3 deficiency blocks microglia-mediated synapse elimination and circuit refinement in the dLGN. The authors further demonstrate that caspase-3 activation mediates synapse loss in AD, loss of caspase-3 prevented synapse loss in AD mice. Overall, this study reveals that caspase-3 activation is an important mechanism underlying the selectivity of microglia-mediated synapse elimination during brain development and in neurodegenerative diseases.*
>
> *Strengths:*
>
> *A previous study (Gyorffy B. et al., PNSA 2018) has shown that caspase-3 signal correlates with C1q tagging of synapses (mostly using in vitro approaches), which suggests that caspase-3 would be an underlying mechanism of microglial selection of synapses for removal. The current study provides direct in vivo evidence demonstrating that caspase-3 activation is essential for microglial elimination of synapses in both brain development and neurodegeneration.*
>
> *The paper is well-organized and easy to read. The schematic drawings are helpful for understanding the experimental designs and purposes.*
>
> *Weaknesses:*
>
> *It seems that astrocytes contain large amounts of engulfed materials from ipsilateral and contralateral axon terminals (Figure S11B) and that caspase-3 deficiency also decreased the volume of engulfed materials by astrocytes (Figures S11C, D). So the possibility that astrocyte-mediated synapse elimination contributes to circuit refinement in dLGN cannot be excluded.*

We would like to clarify that we do not claim that astrocytes are unimportant for synapse elimination or circuit refinement. We acknowledge that the claim made in the original submitted manuscript that caspase-3 does not regulate synapse elimination by astrocytes lacks strong supporting evidence. We have removed this claim and revised the section related to synapse engulfment by astrocytes to provide a more rigorous interpretation of our data. We also removed the section in discussion regarding distinct substrate preferences of microglia and astrocytes.

> *Does blocking single or dual inactivation of synapse activity (using TeTxLC) increase microglial or astrocytic engulfment of synaptic materials (of one or both sides) in dLGN?*

We assume that by “blocking single or dual inactivation of synapse activity”, the reviewer refers to inactivating retinogeniculate synapses from one or both eyes.

We showed that inactivating retinogeniculate synapses from one eye (single inactivation) increases engulfment of inactive synapses by microglia (Figure 6). We did not measure synapse engulfment by microglia while inactivating retinogeniculate synapses from both eyes (dual inactivation). However, based on the total active caspase-3 signal (Figure 2) in the dual inactivation scenario, we do not expect to see an increase in engulfment of synaptic material by microglia.

We did not measure astrocyte-mediated engulfment with single or dual inactivation, as we did not see a robust caspase-3 dependent phenotype in synapse engulfment by astrocytes.

> ***Recommendations for the authors:***
>
> ***Reviewer #1 (Recommendations for the Authors):***
>
> *(1) Figure 1 - It is not clear from this figure whether the authors are measuring caspase 3 in dendritic compartments or in dying relay neurons in the thalamus. The authors state that "either" whole cell death (1B) or smaller punctate signals (1F) were observed. When quantifying "photons" in Figure 1E, it appears most of the signal captured will be of dying relay neurons. What determined which signal was observed, and what is being quantified in Figure 1E? This also applies to the quantifications being reported in Figure 2.*

The quantification includes both types of signals – it is sum of all active caspase-3 signal within the dLGN boundary. We note that there is a significant amount of punctate signal in the TeTxLC-inactivated dLGN. Unfortunately, due to file compression, these signals are not clearly visible in the submitted manuscript file. We have provided high resolution figures in this revision.

As argued above in the response to the public review, apoptotic relay neurons in TeTxLC-inactivated dLGN (not the general thalamus area) occur as a direct consequence of synapse inactivation. Therefore, active caspase-3 signals in these relay neurons should be included in the quantification.

We believe it is the extent of synapse inactivation (i.e., the number of synapses that are inactivated) that determines whether dLGN relay neuron apoptosis occurs or not. Such apoptosis is expected considering the nature of the apoptosis signaling cascade. In the intrinsic apoptosis pathway, release of cytochrome-c from mitochondria induces cleavage of the initiator caspase, caspase-9, and caspase-9 in turn cleaves the executioner caspases, caspase-3/7, which causes apoptosis. Caspase-3 can cleave upstream factors in the apoptosis pathway, leading to explosive amplification of caspase-3 activity (McComb et al., DOI: 10.1126/sciadv.aau9433). When a relay neuron receives a few inactivated synapses, caspase-3 activation in the postsynaptic dendrite can remain local (as we observed in Figure 1), constrained by mechanisms such as proteasomal degradation of cleaved caspase-3 (Erturk et al., DOI: 10.1523/JNEUROSCI.3121-13.2014). However, when a relay neuron receives many inactivated synapses, the cumulative caspase-3 activity induced in the dendrite can overwhelm negative regulation and lead to significantly higher levels of caspase-3 activity in entire dendrites (Figure S4B) through positive feedback amplification, eventually leading to caspase-3 activation in entire relay neurons. Please see line 127-140 and line 403-413 for our discussion in the main text.

> *(2) Figure 5 - Figures 5c-d and Fig 6 are confounded by pseudoreplication, whereby performing statistics on 50-60 microglia inflates statistical significance. Could the*

> *authors show all these data per mouse?*

If we understand the reviewer correctly, the reviewer is suggesting that reporting measurements from multiple microglia in one animal constitutes pseudo-replication. This is correct in a strict sense, as microglia in the same animal are more likely to be similar than microglia from different animals. In the revised version, we have plotted the data by animal in Figure S11 and S13. The observations remain valid. However, we would like to point out that averaging measurements from all microglia in each animal and report by mouse is very conservative, as measurements from microglia in the same animal still vary greatly due to cell-to-cell differences.

> *(3) Although the authors are not the only ones to use this strategy, it is worth noting that performing all microglial experiments in Cx3cr1 heterozygotes could lead to alterations in microglial function that may not be reflective of their homeostatic roles.*

We acknowledge that Cx3cr1 heterozygosity could cause alterations in microglial physiology.

While Cx3cr1 heterozygosity may impact microglia physiology, we note that the engulfment assay in Figure 5 is comparing microglia in *Cx3cr1*$^{+/-}$; *Casp3*$^{+/-}$ and *Cx3cr1*$^{+/-}$; *Casp3*$^{-/-}$ animals. Therefore, the impact of Cx3cr1 heterozygosity is controlled for in our experiment, and the observed difference in engulfed synaptic material in microglia is an effect specific to caspase-3 deficiency. However, we acknowledge that this difference could be quantitatively affected by Cx3cr1 heterozygosity.

It is important to note that we did not perform all microglia engulfment analyses using Cx3cr1$^{+/-}$ mice. We have edited the manuscript to make this more clear. In the activity-dependent microglia engulfment analysis performed in Figure 6, we used *Casp3*$^{+/+}$ and *Casp3*$^{-/-}$ animals and detected microglia with anti-Iba1 immunostaining. Therefore, the impact of Cx3cr1 heterozygosity is not a problem for this experiment.

> *Minor:*
>
> *(1) Figures are presented out of order, which makes the manuscript difficult to follow.*

We have revised text regarding the segregation analysis to align with the order of figures.

> *(2) Figure S3 is very confusing- the terms "left" and "right" are used in three or four partly overlapping contexts (which eye, which injection, which panel or subpanel of the figure is being referred to). Would this not be more appropriately analyzed with a repeated measures ANOVA (multiple comparisons not necessary) rather than multiple separate T-tests?*

We have revised Figure S3 and S5 with better annotation and legends.

Yes, it is possible to use repeated measure two-way ANOVA. The analysis reports significant effect from genotypes, with a dF of 1, SoS and MoS of 0.0001081, $F(1,13) = 7.595$, and $p = 0.0164$. We used multiple separate t-tests because we wanted to show how genotype effects change with increasing thresholds, whereas two-way ANOVA only provides one overall p-value.

> *(3) Could the authors clarify why the percentage overlap (in the controls) is so different between Figure 3C and Figure S3C, and why different thresholds are applied?*

This difference is primary due to difference in age. Figure 3 and Figure S5 are acquired at age of P10, while Figure S3 is acquired at P8. While the segregation process is largely complete by

P8, the segregation continues from P8 to P10. Therefore, overlap measured at P10 will be lower than that measured at P8. If we compare overlap at the same threshold (e.g., 10%) and at the same age in Figure 3 and S5, the overlap is very similar.

The choice of threshold is related to the methods of labeling. In Figure 3, RGC terminals are labeled with AlexaFlour conjugated cholera toxin subunit-beta (CTB). In Figure S3 and S5, RGC axons are labeled by expression of fluorescent proteins. Labeling with CTB only labels membrane surfaces but yields stronger and slightly different signals at fine scales than labeling with fluorescent protein which are cell fillers. For Figure S3 and S5 (which use fluorescent protein labeling), higher thresholds such as those used in Figure 3 (which use CTB labeling) can be applied and the same trend still holds, but the data will be noisier. Regardless of the small difference in thresholds used, the important observation is that the defects in TeTxLC-injected or caspase-3 deficient animals are clear across multiple thresholds.

> *(4) Many describe the eye-specific segregation process as being complete "between P8-10". Other studies have quantified ESS at P10 (Stevens 2007). The authors state they did all quantifications at P8 (l. 82) and refer to Figure 3, but Figure 3 shows images from P10, whereas Figure S3 shows data from P8.*

We did not say we performed all quantification at P8. In line 85, we said “To validate the efficacy of our synapse inactivation method, we injected AAV-hSyn-TeTxLC into the right eye of wildtype E15 embryos and analyzed the segregation of eye-specific territories at postnatal day 8 (P8), when the segregation process is largely complete”. The age of postnatal day 8 in this context is specifically referring to the experiment shown in Figure S3. For the segregation analysis in Figure 3, we specifically stated that the experiment was conducted at P10 (line 277).

Although the experiment in Figure S3 is conducted at P8, and Figure S5 and Figure 3 show results at P10, each dataset always included appropriate age-matched controls. P8 is generally considered an age where segregation is mostly complete and sufficient for us to assess the potency of TeTxLC-delivered AAV on eye segregation. We don’t think performing the experiment shown in Figure S3 at P8 impacts the interpretation of the data.

> *(5) Is Figure 6 also using Cx3cr1 GFP to label microglia? This is not clarified.*

We apologize for this oversight. In Figure 6 microglia are labeled by anti-Iba1 immunostaining. We have clarified this in figure legends and text.

> ***Reviewer #2 (Recommendations for the Authors):***
>
> *(1) The authors quantified the caspase-3 activity using immunostaining and confocal microscopy (Figures 1B-E). They may need to verify the result (increased level of activated caspase-3 upon synapse inactivation) using alternative methods, such as western blotting.*

Both western blot and immunostaining are based on antibody-antigen interaction. These two methods are not likely sufficiently independent. Additionally, to perform a western blot, we would need to surgically collect the TeTxLC-inactivated dLGN to avoid sample contamination from other brain regions. Such collection at the age we are interested in (P5) is very challenging. We have tested the anti-cleaved caspase-3 antibody using caspase-3 deficient mice and we can confirm it is a highly specific antibody that doesn’t generate signal in the caspase-3 deficient tissue samples.

> *(2) Does caspase-3 deficiency alter the density of microglia or astrocytes in dLGN?*

No. Neither the density of microglia nor astrocytes changed with caspase-3 deficiency. In the case of microglia, we find that the mean density of microglia per unit area of dLGN is virtually the same in wild type and caspase-3 deficient mice (two-tailed t test P = 0.8556, 6 wild type and 5 $Casp3^{-/-}$ mice). Some overviews showing microglia in dLGNs of wildtype and caspase-3 deficient mice can be found in Figure S10. Similarly for astrocytes, we did not observe overt changes in astrocytes dLGN density linked to caspase-3 deficiency.

> *(3) During dLGN eye-specific segregation in normal developing animals, did the authors observe different levels of activated caspase-3 in different regions (territories)?*

For normal developing animals, the activated caspase-3 signal is generally sparse, and it is difficult to distinguish whether the signal is related to synapse elimination. For animals receiving TeTxLC-injection, we did notice that in the dLGN contralateral to the injection, where most inactivated synapses are located, the punctate caspase-3 signal tends to concentrate on the ventral-medial side of the dLGN (Figure 1B), which is the region preferentially innervated by the contralateral eye.

> *(4) Recording of NMDAR-mediated synaptic currents may not be necessary for demonstrating that caspase 3 is essential for dLGN circuit refinement. In addition, the PPR may not necessarily reflect the number of innervations that a dLGN neuron receives. Instead, showing the changes in the frequency of mEPSCs (or synapse/spine density) may be more supportive.*

Thank you for the comment. We have performed the suggested mEPSC measurements and reported the results in revised Figure 4D-F.

> *(5) Why is caspase 3 activation enhanced (compared to control) only at 4 months of age, when A-beta deposition has not formed yet, but not at later time points in AD mice (Figure S17)?*

A prevailing hypothesis in the field is that the form of A-beta that is most neurotoxic is the soluble oligomeric form, not the fibril form that leads to plaque deposition. As the oligomeric form appears before plaque deposition, the enhanced caspase-3 activation we observed at 4-month may reflect an increase in oligomeric A-beta, which occurs before any visible A-beta plaque formation.

> *(6) The manuscript can be made more concise, and the figures more organized.*

We removed superfluous details and corrected text-figure mismatches in the revised manuscript to improve readability.

https://doi.org/10.7554/eLife.101779.2.sa0